

Liposomal silibinin as a potential radioprotector of human lymphocytes in the treatment of non-small cell lung cancer

M.H. Nguyen^{1*}, N.D. Pham^{1,2,3#}, Q.T. Che¹, T.H.N. Nguyen⁴, N.B.D. Vu¹,
T.N.M. Tran¹, T.K. Trinh⁵, N.A. Trinh⁶, B.N. Pham¹, V.D. Le⁷

¹Center of Radiation Technology and Biotechnology, Nuclear Research Institute, Dalat city, Lam-dong province, Vietnam

²Laboratory of Tissue Engineering and Biomedical Materials, University of Science, HoChiMinh city, Vietnam

³Vietnam National University, Hochiminh city, Vietnam

⁴Department of Biology, Dalat University, Dalat city, Lam-dong province, Vietnam

⁵Department of Biology and Environment, Yersin University, Dalat city, Lam-dong province, Vietnam

⁶Department of Agriculture and Aquaculture, Tra Vinh University, Tra Vinh province, Vietnam

⁷The Agriculture and Rural Development Department of Tra Vinh

ABSTRACT

► Original article

***Corresponding author:**
Minh-Hiep Nguyen, Ph.D.,
E-mail:
jackminhiep@yahoo.com

Received: May 2021

Final revised: October 2021

Accepted: November 2021

Int. J. Radiat. Res., July 2022;
20(3): 521-529

DOI: 10.52547/ijrr.20.3.1

#Authors equally contributed to this work.

Keywords: Liposomes, lung cancer, radioprotection, radiotherapy, silibinin.

INTRODUCTION

Lung cancer is one of the most prevalent type of cancer. It is responsible for the largest number of deaths by cancer. Although there has been outstanding progress in lung cancer treatment, only approximately 19 % of patients have a 5-year survival⁽¹⁾. Radiotherapy (RT) continues to play an important role in lung cancer treatment. In RT, cancer cells are destroyed by high-energy ionizing rays. However, RT also exhibits negative effects on normal cells or tissues, such as DNA damage, altered cell-cell interactions, prevention of normal cell growth and division, and even cell death⁽²⁾. As a result, the deterioration of patient health leads to a reduction in the effectiveness of RT for cancers^(3,4). In addition, lymphocytes play an important role in the immune system, but they are very vulnerable to ionizing rays

used in RT, and the destruction of lymphocytes during RT negatively affects patient outcomes^(5,6).

Ionizing radiation causes DNA damage and conformational alterations of biomolecules in living organisms⁽⁷⁾. To prevent the effects of radiation, cells generate a lot of specific mechanisms such as free radical scavenging activities, inhibition of lipid peroxidation, and activation of superoxide dismutase (SOD), glutathione peroxidase (GPx), catalase (CAT), and DNA repairs⁽⁸⁾. However, cell damage still occurs if the amount of free radicals exceeds the regulation capacity of the cells. Hence, a compound that promotes the above radioprotective mechanisms of cells will be very useful for radioprotection of normal cells/tissues during RT. On the other hand, radiation-protective agents (radioprotectors) could protect cells against the effect of ionizing radiation via processes including reactive oxygen species (ROS)

scavenging, DNA repair, and activation of the cellular antioxidant signaling pathway ⁽⁹⁾. However, simultaneous radioprotection of normal and cancer cells seems to be unhelpful for RT. Therefore, a compound which not only protects normal cells (such as lymphocytes, skin cells and normal cells of other tissues) from the non-specific effects of RT but simultaneously shows a negligible radioprotective effect on cancer cells or even kills them will be very suitable during RT in cancer patients.

Silibinin (SIL), a bioactive flavonolignan extracted from milk thistle plants, has been known for its pharmacological effects (e.g. hepatoprotective, anti-inflammatory, anti-carcinogenesis), and it has no adverse effects and health hazard ⁽¹⁰⁻¹³⁾. In addition, it has been recently studied as a radioprotector of normal cells (e.g. lymphocytes), but its simultaneous effect on non-small cell lung cancer cells (like A549 cells) under ionizing radiation has not yet been investigated ⁽¹⁴⁾. On the other hand, SIL exhibits poor aqueous solubility (approximately 40 µg/mL), poor absorption and instability in the gastrointestinal tract (only stable in the pH range from 3 to 8), and easy removal from the human body due to various mechanisms like phase II metabolism in the liver, opsonization, etc. ^(15,16). As a result, its oral bioavailability is very low (<1%) ⁽¹⁷⁾, to overcome these problems, SIL has been encapsulated in various nanocarriers such as liposomes, nanoemulsions, solid lipid nanoparticles, nanostructured lipid carriers, nanocomplexes, and polymeric nanoparticles. Liposomes are one of the most suitable nanocarrier systems for SIL due to their high biocompatibility with the human body, ability to enhance the penetration of active compounds through the cell membrane, and nontoxicity or negligible toxicity to humans ⁽¹⁸⁾. In addition, they can be introduced into the body via different routes ⁽¹⁸⁾. Despite this knowledge, the simultaneous evaluation of the radioprotection of liposomal silibinin (Lip-SIL) on human lymphocytes and its effects on human non-small lung cancer cells (like A549 cells) under irradiated condition has not been investigated.

Furthermore, many recent studies related to the application of phytochemicals as radioprotectors in RT mostly focused on the genotoxicity of live cells after irradiation to evaluate (or compare) the radioprotection effectiveness of the phytochemicals. Some common methods used in these studies to investigate the genotoxicity of the cells after ionizing irradiation were chromosomal aberrations, cytokinesis-block micronucleus, comet assays, and γ -H2AX assay ^(14,19). The results in these studies did not mention the amount (or proportion) of cell death after irradiation ^(14,19). Therefore, to comprehensively evaluate whether SIL is suitable for use as a protector against the side effects of RT in cancer patients, a combined method of cell viability assay (for evaluation of the amount of cell death after

irradiation) and cytokinesis-block micronucleus assay (for evaluation of the genotoxicity caused by ionizing rays of the live cells after irradiation) was applied in this study.

Therefore, with the aim to evaluate whether Lip-SIL is suitable for use as a protector against the side effects of RT on human lymphocytes in the treatment of human non-small lung cancer, Lip-SIL was first prepared by the film hydration method combined with sonication; its characteristics (particle size, polydispersity index (PDI), zeta potential, encapsulation efficiency, payload) were then determined. Next, the penetration of Lip-SIL into human lymphocytes and human non-small cell lung cancer cells (A549 cells) was examined by fluorescence microscopy. Finally, simultaneous evaluation of the radioprotection effectiveness of Lip-SIL for human lymphocytes and its effects on non-small cell lung cancer cells (A549 cells) under X-ray irradiated condition was undertaken by using a combined method of cell viability assay and cytokinesis-block micronucleus assay.

MATERIALS AND METHODS

Silibinin (98% purity), Ficoll-Hypaque, and RPMI-1640 medium were obtained from Sigma Aldrich (USA). Phosphatidylcholine (Phospholipon® 90G) was purchased from Lipoid GmbH (Germany). A549 adenocarcinomic human alveolar basal epithelial cells, a gift from University of Medicine and Pharmacy Ho Chi Minh City (Vietnam), were used as a model of non-small cell lung cancer. Whole blood samples were collected from healthy donor volunteers (n=3) at the University of Medicine and Pharmacy, Ho Chi Minh City (Vietnam), according to the Institutional Review Board (IRB) protocols. Other chemicals were of analytical grade.

Preparation of Lip-SIL

Lip-SIL was prepared using a combined method of lipid-film hydration and sonication ⁽⁵⁾. In particular, SIL and phospholipon 90G were solubilized into a mixture of chloroform and methanol (2:1, v/v). The resulting solution was transferred to a round-bottom flask. The solvents were then removed with a rotary vacuum evaporator (IKA RV6, Germany) at 55 °C for 3 hours. Next, the formed lipid film was hydrated by phosphate-buffered saline solution (pH 7.4) for 5 hours to form crude liposomes. Finally, the crude liposomal suspension was reduced in size by sonication using an ultrasonic liquid processor (VC 750, Sonics & Materials, USA). The resulting Lip-SIL suspension was filtered through a cellulose acetate membrane with a pore size of 1.2 µm to remove the unencapsulated SIL particles, and the filtrate was then used for physical characterizations.

Physical characterizations of Lip-SIL

The mean size, polydispersity index (PDI) and zeta potential of Lip-SIL were measured by the Zetasizer Nano ZS (Malvern, U.K.). Briefly, the sample was diluted 100 times with distilled water. The measurement was carried out at a temperature of 25 °C and a detector angle of 173°.

The morphology of Lip-SIL was examined using transmission electron microscopy (TEM) (JEM 1400, JEOL, and Japan). Briefly, approximately 15 µL of the dispersions were dropped onto carbon-coated grids, and the excess was carefully removed with filter paper. Finally, the sample was dried overnight prior to being imaged using TEM.

The encapsulation efficiency and payload of SIL were determined by UV-Vis spectrophotometry (Shimadzu, Japan) at an absorbance wavelength of 287 nm (5, 15). Encapsulation efficiency was determined using equation (1). After preparation, the dispersions were syringe-filtered using a cellulose membrane with a 1.2-µm pore size, then diluted 100 times with 100% ethanol, followed by vortexing. All the mass of SIL recovered from the liposomes was quantified by UV-Vis spectrophotometry. The payload defined in equation (2) was determined by dissolving 2 mg of freeze-dried liposome powders in 2 mL ethanol, followed by vortexing. Finally, the amount of SIL in liposome was also quantified by UV-Vis spectrophotometry.

$$\text{Payload (\%)} = \frac{\text{Amount of silibinin in the liposomes (mg)}}{\text{Amount of liposomal silibinin (mg)}} \times 100 \quad (1)$$

$$\text{Encapsulation efficiency (\%)} = \frac{\text{Amount of silibinin in the liposomes (mg)}}{\text{Initial added amount of silibinin (mg)}} \times 100 \quad (2)$$

The penetration of Lip-SIL into cells

The penetration of Lip-SIL into human blood lymphocytes and human non-small cell lung cancer A549 cells was investigated by a fluorescence microscope (Axio Imager Z2, Carl Zeiss, Germany) equipped with an FITC SP101 filter. Methyl red, a fluorescent dye, was co-encapsulated into Lip-SIL at a ratio of 1:200 (w/w) for observation. The dispersion was filtered for sterilization by cellulose acetate membrane with a pore size of 0.45 µm.

The lymphocytes were incubated in an RPMI-1640 medium supplied with sterile Lip-SIL (containing methyl red), at 37 °C, and 5% CO₂. At a specified amount of time (4, 8 and 16 hours), the cells were washed with PBS and the fluorescent images were captured by fluorescence microscopy under a 20× objective lens.

A549 cells were grown in the RPMI-1640 medium supplied with 10% fetal bovine serum. Between 10⁴ and 10⁵ cells were incubated in a petri dish

containing a glass coverslip and 5% CO₂ at 37 °C (20). When the cells attached to the glass coverslip, the medium was removed and replaced with new RPMI 1640 without fetal bovine serum. The sterile Lip-SIL (containing methyl red) was added to the cultures. At the time points of 4, 8 and 16 hours, the glass coverslip containing the cells was washed 3 times with PBS, and the fluorescent images were captured using fluorescence microscopy under the above-mentioned conditions.

DPPH radical scavenging activity of SIL

The free radical scavenging activity of SIL was evaluated by the DPPH method (21, 22). Briefly, 50 µL of SIL solution in ethanol (1 mg/mL) were added to eppendorf with 1950 µL DPPH solution (0.1 mM, diluted with ethanol), vortexed vigorously, and incubated in the dark for 30 min. After that, the samples were measured by UV-Vis spectrophotometry (Shimadzu, Japan) at an absorbance wavelength of 517 nm. Besides, the radical scavenging activity of SIL was compared with that of curcumin (CUR), which has been reported to have a very high free radical scavenging activity as well as a radioprotection ability. The percentage of the radical scavenging activity of SIL was calculated based on the following equation (3):

$$\text{DPPH scavenging effect (\%)} = \frac{1 - A_{\text{Sample}}}{A_{\text{Control}}} \times 100 \quad (3)$$

where A_{Sample} is the absorbance in the presence of SIL solution mixed with DPPH solution and A_{Control} is the absorbance of DPPH radical solution (without SIL).

Radioprotective activity of Lip-SIL on human lymphocytes

Blood samples from healthy donors—all of whom were non-smokers and had no history of radiation therapy—were collected and kept in lithium heparin tubes. Lymphocytes were isolated by Ficoll-Hypaque according to the manufacturer's protocols. The blood was diluted with Dubeco's phosphate-buffered saline at a ratio of 1:1 (v/v). The blood solution was then layered onto the Ficoll-Hypaque solution. Next, the blood was centrifuged at 400×g for a total of 35 min. The lymphocyte layer was transferred to a new tube, washed twice with PBS, and centrifuged at 240×g for 10 minutes. The supernatant was removed and the cells were resuspended in complete RPMI 1640 at 4°C. The number of cells was counted using a hemocytometer under microscopy (Nikon Eclipse 80i, Nikon, Japan).

The concentration of SIL in the filtered dispersion was determined by UV-Vis spectrophotometry (Shimadzu, Japan). Next, SIL at various concentrations (5, 10, 30 and 50 µg/mL) (in liposomal forms) were added to the RPMI-1640

medium containing the lymphocytes at a cell density of 1×10^6 cells. In this experiment, the sample which was not incubated with nanoformulation was used as the control. All of the samples were incubated overnight in 5% CO₂ at 37 °C. Next, the cells were washed with a fresh RPMI-1640 medium and centrifuged for 10 minutes at 260×g. After that, the sample was irradiated by an X-ray source (Model: Radioflex-200EGM, Rigaku Corporation, Japan) at a 2-Gy dose with a dose rate of 0.45 Gy/min.

The radioprotective activity of Lip-SIL was determined by a combined method of cell viability assay, which was performed to evaluate, using trypan blue, the amount (or proportion) of lymphocyte death after irradiation, and micronucleus (CBMN) assay, which was performed to evaluate the genotoxicity of the live lymphocytes after irradiation (23, 24). Briefly, the above irradiated lymphocytes were incubated, at 37 °C and with 5% CO₂, in a 6-mL RPMI-1640 medium supplemented with 15% heat-inactivated FBS, 1.5% PHA, and Kanamicine sulfate. After 24 hours, a 100-µL cell suspension was collected to assess the cell viability using trypan blue. The percentage of cell death was determined by the equation (4):

$$\text{Percentage of cell death (\%)} = \frac{\text{Total number of dead cells per mL of aliquot}}{\text{Total number of cells per mL of aliquot}} \times 100 \quad (4)$$

Without pause the remaining cell suspension continued to be cultured for 20 hours, and 6 µg/mL of Cytochalasin was added into the cultured samples. Cells were harvested at 72-hour incubation and treated with 0.075-M KCl solution at 4 °C before being fixed with a mixture of methanol and acetic acid (3:1, v/v). Cell suspension was dropped on a clean dry slide and stained with 5% Giemsa solution. Micronuclei analysis was carried out using a Carl Zeiss AXIO Imager Z2 microscope, Metafer 4.0, and MNscore (Metasystem). At least 1000 binuclei cells were scored for counting the micronuclei. It is important to note that the dead cells after irradiation could not continue to grow to become binuclei cells. The frequency of the micronuclei was determined by the equation (5):

$$\text{Micronuclei frequency (\%)} = \frac{\text{Total number of micronuclei in binuclei cells}}{\text{Total number of binuclei cells}} \times 100 \quad (5)$$

In addition, to compare the radioprotective activities of Lip-SIL and liposomal curcumin (Lip-CUR), which is considered a radioprotector (5), the same evaluation methods described above were also used.

Effects of Lip-SIL on A549 cells under irradiated condition

The above combined methods of cell viability

assay and CBMN assay were also used to investigate the effects of Lip-SIL on human non-small cell lung cancer A549 cells.

Briefly, the A549 cells were incubated, at 37 °C and with 5% CO₂, in an RPMI-1640 medium supplemented with 10% fetal bovine serum. At a density of 10^5 cells/flask, the cells were exposed to various concentrations of sterile Lip-SIL (0-50 µg/mL) for 16 hours. The cells were washed with a fresh RPMI-1640 medium and irradiated by an X-ray source at 2 Gy (dose rate of 0.45 Gy/min), while the control flask was not irradiated. Cell viability assay using trypan blue was carried out under the same conditions as mentioned above. CBMN assay was performed for the live (remaining) A549 cells after irradiation. Cytochalasin B solution (6 µg/mL) was added into the flasks containing A549 cells. The cells were continuously incubated for additional 24 hours before being harvested. Microscope slide preparation and micronuclei analysis were carried out using the same protocols as described above.

Statistical analysis

Values are expressed as mean ± standard deviation. In table 1, figure 3, figure 4, and figure 5, the means and standard deviations of the results from at least three independent experiments were calculated using the Microsoft Excel software. In figures 3 to 5, the same superscript letters denote values that were not significantly different according to the one-way ANOVA with the post hoc Tukey test performed using the SPSS software (p<0.05).

RESULTS

Physical characteristics of Lip-SIL

In this study, Lip-SIL was prepared by a combined method of film hydration and sonication. As shown in table 1, the prepared Lip-SIL had a mean particle size of 83.9 ± 2.5 nm, PDI (polydispersity index) of 0.25 ± 0.03 , and zeta potential of -20.6 ± 0.3 mV. The encapsulation efficiency and payload of Lip-SIL were $28.8 \pm 2.0\%$ and $5.1 \pm 0.2\%$, respectively. Moreover, the TEM image indicated that Lip-SIL was spherical, with a nano-size less than 200 nm (figure 1).

Penetration of Lip-SIL into human lymphocytes and A549 cells

In this experiment, methyl red, a fluorescent dye, was co-encapsulated with native SIL into liposomes at a ratio of 1:200 (w/w). Therefore, the fluorescent signals indicated the position of Lip-SIL. As shown in figure 2, green fluorescent signals were detected in lymphocytes (figure 2a) and A549 cells (figure 2b) after they were incubated with Lip-SIL containing methyl red for 4 hours. The fluorescent intensity was stronger after 8 hours and 16 hours of incubation.

Radioprotective activity of Lip-SIL on human lymphocytes

In this experiment, the radioprotective activity of Lip-SIL on human lymphocytes was evaluated by calculating the percentage of cell death and the micronuclei frequency in cells that survived after irradiation by X-ray at a 2-Gy dose with a dose rate of 0.45 Gy/min.

Firstly, as shown in figure 3a, under normal condition (non-irradiated condition), the micronuclei frequency values of the untreated sample and the treated samples at SIL concentrations between 5 and 50 $\mu\text{g}/\text{mL}$ were all less than 1%. On the other hand, the percentages of cell death in the treated samples at SIL concentrations of 5 and 10 $\mu\text{g}/\text{mL}$ were not statistically different from the percentage of cell death in the untreated sample (1.44%). An increase in SIL concentration to 30 and 50 $\mu\text{g}/\text{mL}$ resulted in a sharp increase in the percentage of cell death to 12.85% and 20.73%, respectively.

As shown in figure 3b, under irradiated condition, the percentages of lymphocyte death of the treated samples at SIL concentrations of 5 and 10 $\mu\text{g}/\text{mL}$ decreased approximately by 1.46 and 3.08 times, respectively, compared to the percentage of the untreated sample (17.68%). In addition, the micronuclei frequencies of the treated samples at SIL concentrations of 5 and 10 $\mu\text{g}/\text{mL}$ also decreased by 1.24 and 1.77 times, respectively, compared to that of the untreated sample (23.23%). However, a further increase in the SIL concentration to 30 and 50 $\mu\text{g}/\text{mL}$ led to a 1.98- and 4-fold increase, respectively, in the percentage of cell death, and a 1.35- and 1.46-fold increase, respectively, in the micronuclei frequency, compared to the corresponding values of the treated sample at a SIL concentration of 10 $\mu\text{g}/\text{mL}$.

To better understand the radioprotective mechanisms of Lip-SIL, the radioprotective and free radical scavenging activities of Lip-SIL and Lip-CUR (liposomal curcumin) are compared in the supplementary data (Supplemental figure S1) and figure 4. As shown in figure S1a, under non-irradiated condition, the micronuclei frequencies of the samples treated with Lip-CUR at CUR concentrations from 0 to 50 $\mu\text{g}/\text{mL}$ were less than 1% and, thus, not statistically different; the treatment at CUR concentrations more than 10 $\mu\text{g}/\text{mL}$ resulted in a significant increase in the percentage of lymphocyte death. Meanwhile, under X-ray irradiated condition at a dose of 2 Gy (figure S1b), the percentage of lymphocyte death and the micronuclei frequency of the sample treated with Lip-CUR at a CUR concentration of 10 $\mu\text{g}/\text{mL}$ were 13.46% and 18.52%, respectively, while those of the control (untreated sample) were 17.68% and 23.23%, respectively. On the other hand, as shown in figure 4b, under irradiated condition at a dose of 2 Gy, compared to the control (untreated sample), the treatment with Lip-CUR at a CUR concentration of 10

$\mu\text{g}/\text{mL}$ resulted in a considerable decrease in the percentage of lymphocyte death from 17.68% to 13.46%, as well as in the micronuclei frequency from 23.23% to 18.52%. Besides, the percentage of lymphocyte death and the micronuclei frequency of the sample treated with Lip-SIL at a SIL concentration of 10 $\mu\text{g}/\text{mL}$ were only 5.75% and 13.07%, respectively. On the other hand, as shown in figure 4a, the ROS scavenging activity of SIL was extremely low (3.43%), while that of CUR was more than 30%.

Effects of Lip-SIL and radiation on A549 cells

As shown in figure 5a, under normal condition (non-irradiated condition), the percentage of cell death and the micronuclei frequency in all samples (treated and untreated) were less than 3.3% and 2.4%, respectively, and there was no statistically significant difference between the values. Under X-ray irradiation at a dose of 2 Gy (figure 5b), the percentages of cell death were statistically equal across the samples, but they were 2.3- to 3.5-fold higher than the percentages under non-irradiated condition. In addition, the micronuclei frequencies increased by 10 to 18 times under irradiated condition compared to those of the corresponding samples under non-irradiated condition (figure 5a). Under irradiated condition, the micronuclei frequencies of the treated samples at SIL concentrations of 10, 30 and 50 $\mu\text{g}/\text{mL}$ were 21.38%, 20.78% and 23.43%, respectively, compared to a frequency of 17.69% for the untreated sample.

Table 1. Physical characteristics of liposomal silibinin (n=3).
Lip-SIL: liposomal silibinin; mV: milivolt; nm: nanometer.

	Mean size (nm)	Polydispersity index	Zeta potential (mV)	Encapsulation efficiency (%)	Payload (%)
Lip-SIL	83.9 \pm 2.5	0.25 \pm 0.03	-20.6 \pm 0.3	28.8 \pm 2.0	5.1 \pm 0.2

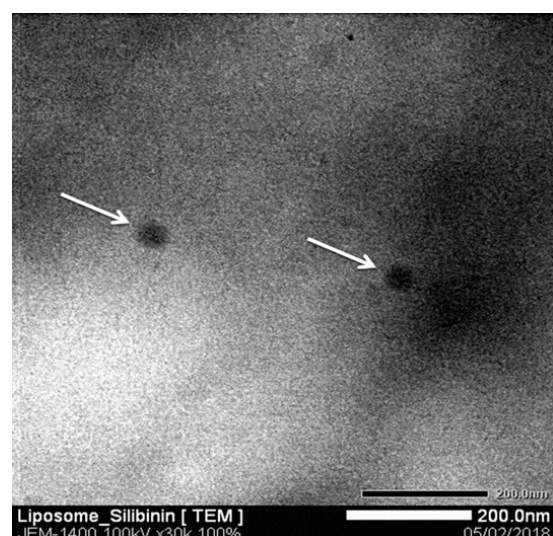


Figure 1. TEM image of Lip-SIL pointed out by the white arrows. Magnification: 30000 times. Arrows indicate the positions of Lip-SiL.

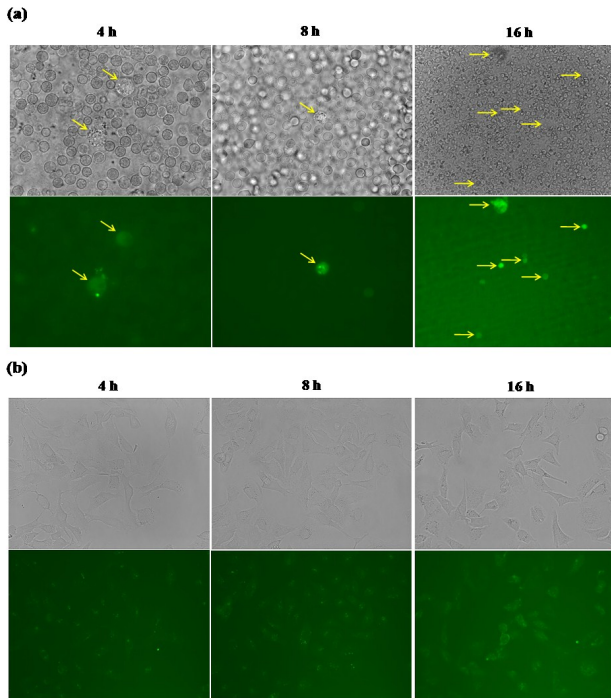


Figure 2. Fluorescence images of penetration of Lip-SIL into (a) human blood cells and (b) A549 human lung cancer cells. Magnification: 200 times. Arrows indicate the positions of lymphocytes and green fluorescent signals indicate the positions of Lip-SIL.

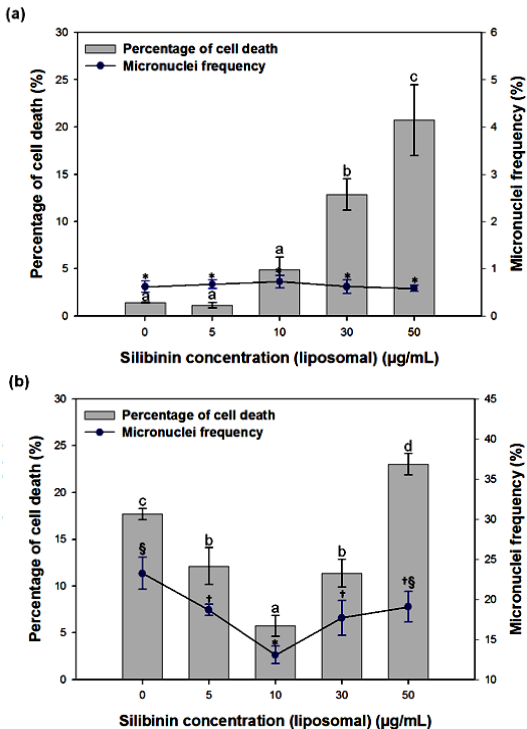


Figure 3. Radioprotective activity of Lip-SIL expressed in terms of the percentage of cell death and the micronuclei frequency of human lymphocytes at an X-ray radiation dose of (a) 0 Gy (no irradiation), and (b) 2 Gy. Any two mean values followed by the same superscript letter represent two non-statistically different values, according to the post hoc Tukey test ($p < 0.05$).

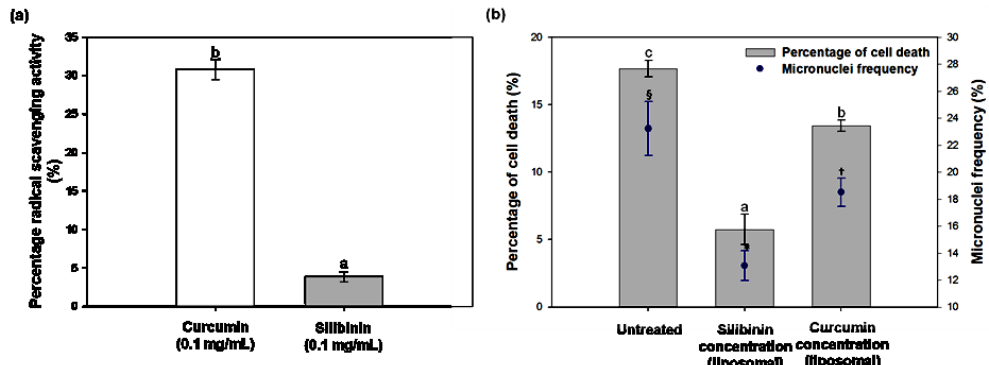


Figure 4. Comparison of Lip-SIL and Lip-CUR, at the optimum concentration, in terms of (a) the DPPH radical scavenging activity and (b) the percentage of cell death and the micronuclei frequency of human lymphocytes at an X-ray radiation dose of 2 Gy. Any two mean values followed by the same superscript letter represent two non-statistically different values, according to the post hoc Tukey test ($p < 0.05$).

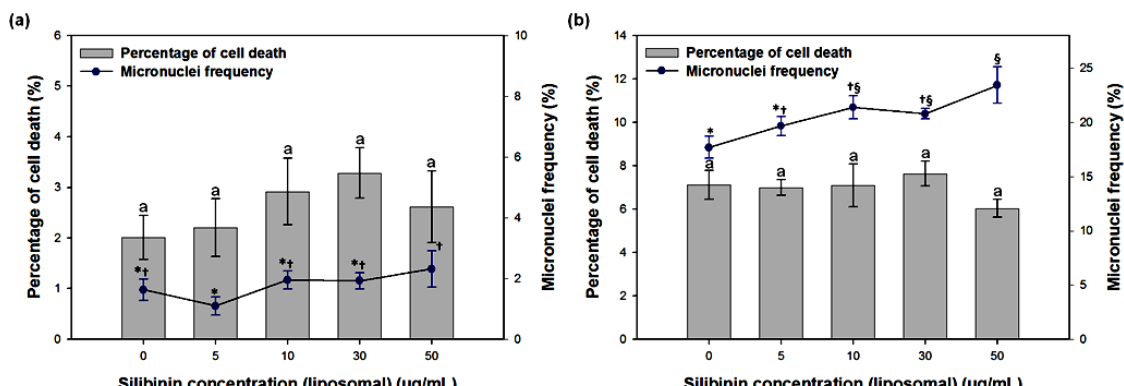


Figure 5. Effects of Lip-SIL on A549 cells expressed in terms of the percentage of cell death and the micronuclei frequency of A549 cells at an X-ray radiation dose of (a) 0 Gy (i.e. no irradiation), and (b) 2 Gy. Any two mean values followed by the same superscript letter represent two non-statistically different values, according to the post hoc Tukey test ($p < 0.05$).

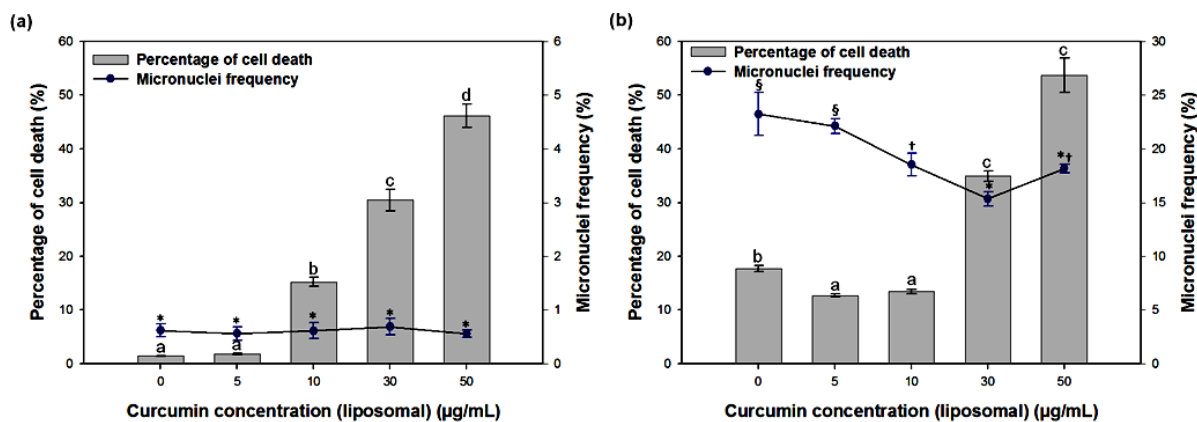


Figure S1. The radioprotective activity of the Lip-CUR as expressed in terms of the percentage of cell death and the micronuclei frequency of human lymphocytes upon X-ray radiation dose of (a) 0 Gy (i.e. no irradiation), and (b) 2 Gy. Any two mean values that were followed by the same superscript letter represented two non-statistically different values according to the post-hoc Tukey test ($p < 0.05$).

DISCUSSION

Lip-SIL was successfully prepared, with good physical characteristics (small particle size, small polydispersity index, and high zeta potential), by a combined method of film hydration and sonication (table 1). In addition, the zeta potential (-20.6 mV) indicated a relative stability of Lip-SIL due to repulsive electrostatic forces between the nanoparticles (5). The payload of Lip-SIL ($5.1 \pm 0.2\%$) was similar to that obtained by Ochi *et al.* (25). TEM image re-affirmed the formation of Lip-SIL (figure 1). All the above results indicated that the prepared Lip-SIL was suitable for the subsequent *in vitro* experiments on human lymphocytes and A549 cells.

As shown in figure 2, after the lymphocytes were incubated for 4 hours with Lip-SIL co-encapsulated with methyl red as fluorescent dye, green fluorescent signals were clearly detected in lymphocytes (figure 2a) and A549 cells (figure 2b), indicating the quick penetration of Lip-SIL into these cells. After incubation for a longer time, stronger fluorescent signals indicated that a higher amount of Lip-SIL had penetrated these cells. The fluorescent signals were only detected in lymphocytes (indicated by arrows in figure 2a) but not in the red blood cells. This was because the nanoparticles (such as nanoliposomes) could penetrate the cells by many pathways, with endocytosis the most important (26, 27), and the erythrocyte membrane skeleton had been reported to inhibit nanoparticle endocytosis (28).

In this study, the radioprotective activity of Lip-SIL on human lymphocytes was evaluated by a combined method of cell viability assay and cytokinesis-block micronucleus assay. In this method, the percentages of cell death and the micronuclei frequencies of cells of the treated and untreated samples that survived under normal (non-irradiated) and irradiated conditions were determined and compared. In addition, it is important to note that the radioprotective activity of the natural compound (liposomal form) was independent of the blood

donors, and this was demonstrated by the statistical results analyzed by two-way ANOVA with the post-hoc Tukey test ($p < 0.05$) in our previous study (5). Particularly, under normal condition (non-irradiated condition), Lip-SIL caused no significant genotoxicity to human lymphocytes, and it only exhibited a considerable cytotoxic effect at SIL concentrations over 10 $\mu\text{g}/\text{mL}$ (figure 3a). However, under irradiated condition (figure 3b), the percentage of cell death and genotoxicity on lymphocytes significantly decreased in the presence of Lip-SIL, compared to the control (untreated sample). In this experiment (figure 3b), the percentage of lymphocyte death was the total of the percentage of cell death caused by the cytotoxicity of Lip-SIL itself under non-irradiated condition (figure 3a) and the percentage of cell death caused by X-ray irradiation. Lip-SIL at a SIL concentration of 10 $\mu\text{g}/\text{mL}$ showed a negligible genotoxic effect and slight cytotoxicity (4.93%) under non-irradiated condition (figure 3a), but it exhibited the highest radioprotection for lymphocytes against X-ray irradiation (figure 3b). A further increase in SIL concentration to 30 and 50 $\mu\text{g}/\text{mL}$ resulted in lower radioprotection for lymphocytes. It could be explained by the cytotoxicity of SIL at a higher concentration and the excessive presence of an exogenous antioxidant (like SIL) can result in cytotoxicity or even act as a radiation sensitizer (29-31). These results are similar to that reported by Tiwari *et al.*, who also found that SIL had a radioprotective effect on human lymphocytes against ionizing rays (14). In this study, although human lymphocytes were pretreated with native SIL (crude form) at an optimal concentration of 200 μM (corresponding to 96.488 $\mu\text{g}/\text{mL}$) before gamma irradiation at a dose of 3 Gy, the micronuclei frequency of the treated samples only decreased by approximately 30% compared to that of the untreated sample. However, in our study, by pretreating the lymphocytes with Lip-SIL at a SIL concentration of 10 $\mu\text{g}/\text{mL}$ before irradiation, their micronuclei frequency significantly decreased by

43.76% compared to that of the untreated sample. Therefore, it is clear that by using SIL in a nanoliposomal form, a higher radioprotection for human lymphocytes could be achieved at a much lower SIL concentration compared to using SIL in the native form.

In addition, although the ROS scavenging activity of SIL was extremely low (3.43%) and approximately 9 times lower than that of CUR (figure 4a), the radioprotective activity of Lip-SIL was significantly higher than that of Lip-CUR (at the same concentration of 10 $\mu\text{g}/\text{mL}$) (figure 4b). This implies that the radioprotective activity of Lip-SIL is mostly based on various mechanisms of intracellular activations that protect cells against damage caused by ROS (generated by ionizing rays), such as inhibition of lipid peroxidation and activation of superoxide dismutase (SOD), glutathione peroxidase (GPx), and catalase (CAT)^(8,32). For example, Zhou *et al.* found that the presence of SIL in cardiac myocytes enhanced the SOD activity, which neutralizes superoxide anions and reduces lipoperoxide production⁽³³⁾. This probably explains why Lip-SIL exhibited a higher radioprotective activity, compared to Lip-CUR, although its free radical scavenging activity was significantly lower. From these results, it is clear that the radioprotective effect of bioactive compounds does not solely depend on the free radical scavenging activity but also on their ability to activate cellular mechanisms.

For A549 cancer cells, under normal condition (non-irradiated condition), the presence of Lip-SIL at a SIL concentration of less than 50 $\mu\text{g}/\text{mL}$ exhibited no significant effect on cytotoxicity and genotoxicity. However, exposure to X-ray at a dose of 2 Gy led to a significant increase (2.3- to 3.5-fold) in cytotoxicity and genotoxicity in all treated and untreated samples (figure 5b). It is clear that under the same condition (non-irradiated condition or irradiated condition), there was no statistical difference in the percentages of cell death between the samples. However, at a SIL concentration of more than 5 $\mu\text{g}/\text{mL}$, Lip-SIL enhanced genotoxicity in A549 cancer cells under X-ray irradiated condition (figure 5b). The results in figure 5a and figure 5b demonstrate that under irradiated condition, Lip-SIL not only exhibited no radioprotective effect on A549 cells against X-ray irradiation, but also caused considerable genotoxicity.

By combining the results from figure 3 to Figure 5, it is obvious that Lip-SIL at a SIL concentration of 10 $\mu\text{g}/\text{mL}$ had a maximum radioprotective effect on human lymphocytes against X-ray irradiation, but showed no radioprotective effect on, or even increased genotoxicity in, human non-small lung cell cancer A549 cells. In previous studies, SIL was also reported to be able to suppress proliferation and promote apoptosis of A549 cells due to the downregulation of rhomboid domain-containing

protein 1 (RHBDD1)^(34,35). Therefore, Lip-SIL at a SIL concentration of 10 $\mu\text{g}/\text{mL}$ is very suitable for use as a radioprotector in RT treatment of non-small cell lung cancer.

CONCLUSION

In summary, Lip-SIL was successfully prepared, with good physical characteristics and a spherical shape, by a combined method of film hydration and sonication. The quick penetration of Lip-SIL into human lymphocytes and A549 human non-small lung cancer cells were well visualized by fluorescence microscopy. Lip-SIL showed the highest radioprotection for human lymphocytes against X-ray irradiation at a SIL concentration of 10 $\mu\text{g}/\text{mL}$, but showed no radioprotective activity or even increased genotoxicity in human lung cancer A549 cells. Therefore, Lip-SIL has a great potential for wide application in protection of lymphocytes in RT treatment for lung cancer. Moreover, the findings of this study also demonstrate that the radioprotective effect of a bioactive compound does not solely depend on its free radical scavenging activity but also on its ability to activate cellular mechanisms.

ACKNOWLEDGEMENT

The authors would like to acknowledge the research funding from Nuclear Research Institute and Vietnam Atomic Energy Institute (Grant number: 12/HD/ĐTCB) and to thank Institute of Developmental Philosophy (Vietnam) for the contribution to this work.

Conflicts of interest: On behalf of all authors, the corresponding author states that there is no conflict of interest.

Funding: This study was funded by Nuclear Research Institute and Vietnam Atomic Energy Institute (Grant number: 12/HD/ĐTCB) and Institute of Developmental Philosophy (Vietnam).

Ethics approval: Not applicable.

Author contributions: MHN, NDP and QTC conceived and designed the article. The experiments were carried out by QTC, THNN, NBDV, BNP and TNMT. Data curation and analysis were done by MHN, NDP, TTK, VDL and NAT. Writing of the entire manuscript was done by MHN and THNN. All the authors have read, revised and approved the manuscript.

REFERENCES

1. Siegel RL, Miller KD, Jemal A (2020) Cancer statistics, 2020. *CA Cancer J Clin*, **70**: 7-30.
2. Azzam EI, Jay-Gerin JP, Pain D (2012) Ionizing radiation-induced metabolic oxidative stress and prolonged cell injury. *Cancer Lett*, **327**: 48-60.
3. Abratt RP and Morgan GW (2002) Lung toxicity following chest

irradiation in patients with lung cancer. *Lung Cancer*, **35**: 103-109.

- Kong FM, Hayman JA, Griffith KA, Kalemkerian GP, Arenberg D, Lyons S, Turrissi A, Lichter A, Fraass B, Eisbruch A, Lawrence TS, Haken RKT (2006) Final toxicity results of a radiation-dose escalation study in patients with non-small-cell lung cancer (NSCLC): predictors for radiation pneumonitis and fibrosis. *Int J Radiat Oncol Biol Phys*, **65**: 1075-1086.
- Nguyen MH, Duy PN, Dong B, Nguyen THN, Bui CB, Hadinoto K (2017) Radioprotective activity of curcumin-encapsulated liposomes against genotoxicity caused by gamma Cobalt-60 irradiation in human blood cells. *Int J Radiat Biol*, **93**: 1267-1273.
- Xie X, Gong S, Jin H, Yang P, Xu T, Cai Y, Guo C, Zhang R, Lou F, Yang W, Wang H (2020) Radiation-induced lymphopenia correlates with survival in nasopharyngeal carcinoma: impact of treatment modality and the baseline lymphocyte count. *Radiat Oncol*, **15**: 65.
- Yamamori T, Yasui H, Yamazumi M, Wada Y, Nakamura Y, Nakamura H, Inanami O (2012) Ionizing radiation induces mitochondrial reactive oxygen species production accompanied by upregulation of mitochondrial electron transport chain function and mitochondrial content under control of the cell cycle checkpoint. *Free Radical Biol Med*, **53**: 260-270.
- Li L, Zeng J, Gao Y, He D (2010) Targeting silibinin in the antiproliferative pathway. *Expert Opin Investig Drugs*, **19**: 243-255.
- Aprotosoaie AC, Trifan A, Gille E, Petreus T, Bordeianu G, Miron A (2015) Can phytochemicals be a bridge to develop new radioprotective agents?. *Phytochem Rev*, **14**: 555-566.
- Gupta OP, Sing S, Bani S, Sharma N, Malhotra S, Gupta BD, Banerjee SK, Handa SS (2000) Anti-inflammatory and anti-arthritis activities of silymarin acting through inhibition of 5-lipoxygenase. *Phytomedicine*, **7**: 21-24.
- Singh RP, Deep G, Chittezhath M, Kaur M, Dwyer-Nield LD, Mankinson AM, Agarwal R (2006) Effect of silibinin on the growth and progression of primary lung tumors in mice. *J Natl Cancer Inst*, **98**: 846-855.
- Naso LG, Ferrer EG, Butenko N, Cavaco I, Lezama L, Rojo T, Etcheverry SB, Williams PAM (2011) Antioxidant, DNA cleavage, and cellular effects of silibinin and a new oxovanadium (IV)/Silibinin complex. *J Biol Inorg Chem*, **16**: 653-668.
- Mateen S, Raina K, Agarwal R (2013) Chemopreventive and anti-cancer efficacy of SIL against growth and progression of lung cancer. *Nutr Cancer*, **65**: 3-11.
- Tiwari P, Kumar A, Ali M, Mishra KP (2010) Radioprotection of plasmid and cellular DNA and Swiss mice by silibinin. *Mutat Res*, **695**: 55-60.
- Nguyen HM, Yu H, Dong B, Hadinoto K (2016) A supersaturating delivery system of silibinin exhibiting high payload achieved by amorphous nano-complexation with chitosan. *Eur J Pharm Sci*, **89**: 163-171.
- Wu JW, Lin LC, Hung SC, Chi CW, Tsai TH (2007) Analysis of silibinin in rat plasma and bile for hepatobiliary excretion and oral bioavailability application. *J Pharm Biomed Anal*, **45**: 635-641.
- Fatehi D, Mohammadi M, Shekarchi B, Shabani A, Seify M, Rostamzadeh A (2018) Radioprotective effects of Silymarin on the sperm parameters of NMRI mice irradiated with gamma-rays. *J Photochem Photobiol B*, **178**: 489-495.
- Lutsenko SV, Gromovskykh TI, Krasnyuk II, Vasilenko IA, Feldman NB (2018) Antihapatotoxic activity of Liposomal silibinin. *Bionanosci*, **8**: 581-586.
- Redon CE, Dickey JS, Bonner WM, Sedelnikova OA (2009) γ -H2AX as a biomarker of DNA induced by ionizing radiation in human peripheral blood lymphocytes and artificial skin. *Adv Space Res*, **43**: 1171-1178.
- Whitlon DS, Baas PW (1992) Improved methods for using glass coverslips in cell culture and electron microscopy. *J Histochem Cytochem*, **40**: 875-877.
- Ak T and Gülcin I (2008) Antioxidant and radical scavenging properties of curcumin. *Chem Biol Interact*, **174**: 27-37.
- Gülcin I (2007) Comparison of *in vitro* antioxidant and antiradical activities of L-tyrosine and L-Dopa. *Amino Acids*, **32**: 431-438.
- Fenech M (2010) The lymphocytes cytokinesis-block micronucleus cytome assay and its application in radiation biodosimetry. *Health Phys*, **98**: 234-243.
- Strober W (2015) Trypan blue exclusion test of cell viability. *Curr Protoc Immunol*, **111**: A3.B.1-A3.B.3.
- Ochi AM, Amoabediny G, Rezayat S, Akbarzadeh A, Ebrahimi B (2015) Design and preparation of encapsulated nano-liposome controlled release including silibinin anti-cancer herbal drug (nano phytosome). *JSSU*, **23**: 2000-2012.
- Ducat E, Evrard B, Peulen O, Piel G (2011) Cellular uptake of liposomes monitored by confocal microscopy and flow cytometry. *J Drug Del Sci Tech*, **21**: 469-477.
- Jian Y, Azadeh B, Geert D, Jeroen B, René CLO, Alexander K (2016) Drug delivery via cell membrane fusion using lipopeptide modified liposomes. *ACS Cent Sci*, **2**: 621-630.
- Gao X, Yue T, Tian F, Liu Z, Zhang X (2017) Erythrocyte membrane skeleton inhibits nanoparticle endocytosis. *AIP Adv*, **7**: 065303.
- Amiri B, Ebrahimi-Far M, Saffari Z, Akbarzadeh A, Soleimani E, Chiani M (2016) Preparation, characterization and cytotoxicity of silibinin containing nanoniosomes in T47 human breast carcinoma cells. *Asian Pac J Cancer Prev*, **17**: 3835-3838.
- Poljsak B, Sutup D, Milišav I (2013) Achieving the balance between ROS and antioxidants: when to use the synthetic antioxidants. *Oxid Med Cell Longev*, **956792**.
- Nambiar DK, Rajamani P, Deep G, Jain AK, Agarwal R, Singh RP (2015) Silibinin preferentially radiosensitizes prostate cancer by inhibiting DNA repair signaling. *Mol Cancer Ther*, **14**: 2722-2734.
- Loguercio C and Festi D (2011) Silybin and the liver: From basic research to clinical practice. *World J Gastroenterol*, **17**: 2288-2301.
- Zhou B, Wu LJ, Tashiro S, Onodera S, Uchiimi F, Ikejima T (2006) Silibinin protects rat cardiac myocyte from isoproterenol-induced DNA damage independent on regulation of cell cycle. *Biol Pharm Bull*, **29**: 1990-1995.
- Xu S, Zhang H, Wang A, Ma Y, Gan Y, Li G (2020) Silibinin suppresses epithelial-mesenchymal transition in human non-small cell lung cancer cells by restraining RHBDD1. *Cell Mol Biol Lett*, **25**: 36.
- Zhang X, Zhao Y, Wang C, Ju H, Liu W, Zhang X, Miao S, Wang L, Sun Q, Song W (2018) Rhomboid domain-containing protein 1 promotes breast cancer progression by regulating the p-Akt and CDK2 levels. *Cell Commun Signal*, **16**: 65.

